Ionic Determinants of Conduction Velocity Drop and Propagation Failure During Pacing Stress Protocols

Alejando Liberos[1], Hector Martinez-Navarro[1], Duna de Luis-Moura[1], Saman Golmaryami[2], María Termenón-Rivas[1], Giada S Romitti[1], Ignacio García-Fernández[1], Miguel Lozano[1], Etel Silva[2], Juan Fernandez-Armenta[2], Miguel Rodrigo[1]

[1]CoMMLab, Departament d'Enginyeria Electrònica, Departament d'Informàtica, Universitat de València, València, España
[2]Department of Cardiology, Hospital U. Puerta del Mar, Cádiz, Spain

Abstract

Functional pacing protocols using progressively premature stimuli have been proposed to identify arrhythmogenic atrial substrate.

We used a population of 2,100 human atrial models with independently varied ionic conductances to investigate conduction responses during premature stimulation. After physiological filtering, 1,668 models were analyzed and classified into preserved conduction (NonDropPop), conduction slowing (DropPop), or propagation failure (FailPop). Steady-state conduction velocity was primarily determined by g_{Na}, whereas the response to premature stimulation was most strongly associated with g_{K1}. Within DropPop, the additional conduction slowing as propagation failure was approached involved both g_{K1} and g_{Na} with a smaller contribution from g_{CaL}. DropPop models exhibited reduced g_{Na} together with increased g_{CaL} and j_{Rel}, whereas FailPop was characterized by markedly reduced g_{K1} with increased g_{CaL}, I_{NCX} and g_{Ks}.

These findings identify distinct ionic signatures associated with conduction slowing and propagation failure, supporting future investigation of heterogeneous tissue as a mechanism underlying abnormal conduction during functional pacing protocols.

1. Introduction

Atrial fibrillation (AF) is the most common sustained cardiac arrhythmia and is associated with disorganised electrical activation of the atria. Functional pacing protocols have emerged as a promising approach to uncover latent electrophysiological abnormalities that are not apparent during conventional pacing [1,2].

In particular, protocols based on a sequence of premature stimuli delivered at progressively shorter coupling intervals have been increasingly explored in the clinical setting. By challenging the atrial substrate close to its refractory period, these protocols frequently elicit highly fractionated electrograms that are not observed during conventional pacing. These functional electrogram abnormalities have been proposed as markers of the arrhythmogenic substrate and may help guide catheter ablation [3].

Although fractionated electrograms are readily observed during these pacing protocols, the electrophysiological mechanisms responsible for their appearance remain poorly understood. Premature stimulation may expose underlying functional heterogeneities that become evident only when the tissue is challenged close to its refractory period. At short coupling intervals, some regions may exhibit conduction slowing or local propagation failure, resulting in wavefront discontinuities that may contribute to the generation of complex electrogram patterns.

The mechanisms underlying this response may involve structural remodeling as well as intrinsic electrophysiological differences between atrial regions. In this work, we used a computational population of atrial electrophysiological models spanning a wide range of ionic profiles. By comparing models exhibiting preserved conduction, conduction slowing, or propagation failure during progressively premature stimulation, we identified the ionic determinants associated with these distinct conduction behaviours.

2. Methods

2.1. Electrophysiological tissue model and population generation

Electrophysiological simulations were performed using the baseline human atrial model proposed by Koivumäki et al. [4].

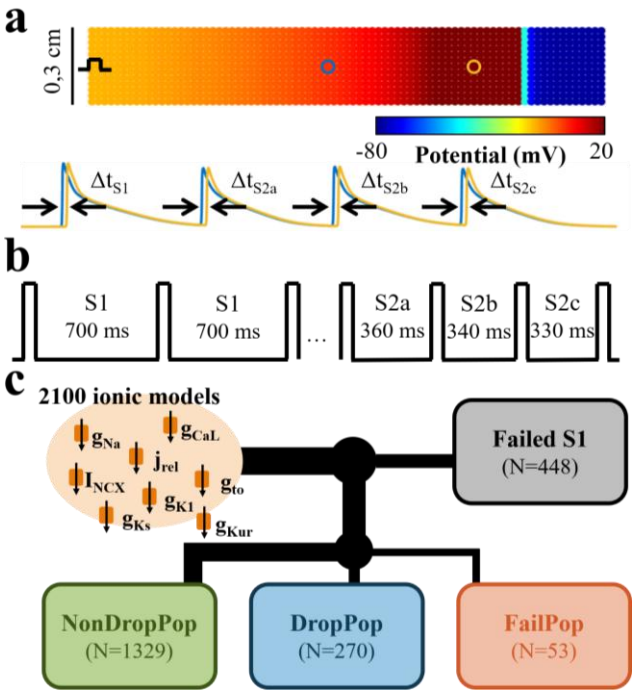

Figure 1. Methodology employed. (a) Geometrical model. Conduction velocity (CV) was calculated from activation times measured at two recording sites. (b) Stimulation protocol consisting of seven conditioning stimuli (S1) followed by three premature stimuli (S2a-S2c). (c) Population classification workflow. Of the 2100 generated ionic models, in which eight ionic parameters were scaled, those that failed to propagate conditioning stimuli were excluded. The remaining models were classified as NonDropPop (all premature stimuli propagated without CV reduction), DropPop (all premature stimuli propagated with CV reduction), or FailPop (failure to propagate one or more premature stimuli).

To reproduce inter-subject electrophysiological variability, a population of 2,100 ionic profiles was generated by scaling eight major ionic conductances and transport mechanisms (g_{Na}, g_{CaL}, j_{rel} – RyR mediated sarcoplasmic reticulum Ca^{2+} release-, I_{NCX}, g_{K1}, g_{to}, g_{Ks}, g_{Kur}). Scaling factors were sampled between −50% and +100% of their baseline values using Latin Hypercube Sampling (LHS) [5,6]. This approach provides a uniform exploration of the multidimensional ionic parameter space while avoiding clustering of sampled combinations.

Each ionic profile was incorporated into a one-dimensional homogeneous tissue strand measuring 0.3 × 2 × 0.025 cm, discretized with an inter-node distance of 0.25 mm. Electrical propagation was simulated using the monodomain formulation assuming isotropic diffusion. The diffusion coefficient was adjusted so that the baseline model reproduced a conduction velocity of 62.5 cm/s under steady-state pacing.

2.2. Stimulation protocol and conduction analysis

Each tissue model was paced from one end using a stimulation protocol designed to evaluate conduction under progressively shorter coupling intervals. Seven conditioning stimuli (S1) were delivered at a basic cycle length (BCL) of 700 ms, followed by three premature stimuli (S2a, S2b and S2c) with coupling intervals of 360, 340 and 330 ms, respectively (Figure 1). These coupling intervals were selected based on the approximate effective refractory period of the baseline tissue, remaining slightly above this threshold [3].

Conduction velocity (CV) was calculated for each successfully propagated stimulus from activation times measured at two locations along the tissue strand, positioned 0.975 cm and 1.725 cm from the stimulation site (Figure 1). These locations were selected to avoid the influence of stimulus-induced local effects and boundary conditions on CV estimation.

Only ionic profiles that successfully propagated all conditioning stimuli were included in the premature stimulation analysis. These profiles were subsequently classified according to their response to the premature stimuli. Models with successful propagation of all premature stimuli without a reduction in CV were classified as *NonDropPop*. Models exhibiting successful propagation of all premature stimuli together with any measurable decrease in conduction velocity between S2a and S2c were classified as *DropPop*. Finally, models in which at least one premature stimulus failed to propagate across the tissue strand were classified as *FailPop*.

Differences in ionic scaling factors between groups were assessed using the Mann–Whitney U test. Statistical significance was established at $p < 0.05$.

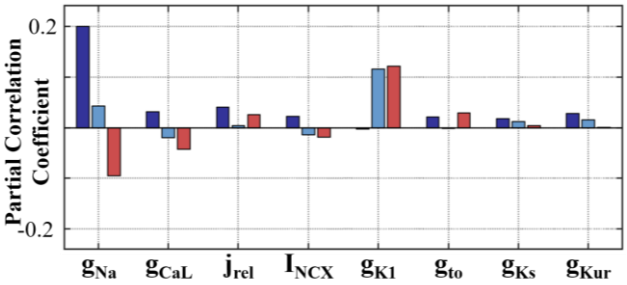

Figure 2. Partial correlation coefficients between ionic scaling factors and conduction velocity (CV) metrics. Dark blue bars represent CV during steady-state pacing (S1), light blue bars represent the relative CV reduction between S1 and the first premature stimulus (S2a), calculated as $(CV_{S2a}-CV_{S1})/CV_{S1}$, and dark red bars represent the relative CV reduction between S2a and S2c within the DropPop population, calculated as $(CV_{S2c}-CV_{S2a})/CV_{S2a}$.

3. Results

3.1. Population response to premature stimulation

A total of 2,100 ionic profiles were simulated. Of these, 448 failed to successfully propagate conditioning stimuli and were excluded from further analysis. The remaining 1,652 models were classified according to their response to premature stimulation into *NonDropPop* (n = 1329), *DropPop* (n = 270) and *FailPop* (n = 53).

The baseline model exhibited a conduction velocity of 62.5 cm/s during steady-state pacing and a constant conduction velocity of 57.7 cm/s during premature stimulation (S2a, S2b and S2c) and was therefore classified as NonDropPop. Conduction velocity during steady-state pacing was 66.5±13.1 cm/s, 59.0±16.3 cm/s and 48.6±21.5 cm/s for NonDropPop, DropPop and FailPop, respectively.

During premature stimulation, CV in NonDropPop models was 64.0±13.7 cm/s, whereas DropPop models exhibited a CV of 56.3±26.9 cm/s during S2a, decreasing by 5.3±5.2 cm/s at S2c.

Conduction velocity determinants were further investigated by analysing the relationship between ionic scaling factors and CV dynamics (Figure 2). Partial correlation analysis identified the main ionic determinants of conduction velocity during steady-state pacing, as well as of the relative CV reduction between steady-state pacing and the first premature stimulus, defined as $(CV_{S2a} - CV_{S1})/ CV_{S1}$.

As expected, steady-state CV was primarily associated with g_{Na} (partial r=0.201). In contrast, the relative CV reduction during premature stimulation showed the strongest association with g_{K1} (partial r=0.116), with smaller contributions from g_{Na} (partial r=0.043) and g_{CaL}(partial r=-0.02).

Within the DropPop population, partial correlation analysis was further performed to identify the ionic determinants of the additional conduction slowing observed during premature stimulation. The relative CV reduction between S2a and S2c, defined as $(CV_{S2c} - CV_{S2a})/ CV_{S2a}$, was correlated with ionic scaling factors. The strongest associations were observed for g_{K1} (partial r=0.121), g_{Na} (partial r=-0.096) while g_{CaL} exhibited a weaker negative association (partial r=-0.043).

Figure 3 summarizes the distribution of ionic scaling factors across the *NonDropPop*, *DropPop* and *FailPop* populations. Compared with *NonDropPop*, *DropPop* models exhibited reduced g_{Na} together with increased g_{CaL} and j_{Rel} whereas a modest reduction in g_{K1} was also observed. In contrast, *FailPop* models were characterized by increased g_{CaL}, I_{NCX} and g_{Ks}, together with reduced g_{K1} ($p < 0.05$ for all comparisons). These findings suggest that conduction slowing and propagation failure are associated with distinct ionic remodeling profiles, with increased g_{CaL} representing the only alteration common to both populations.

4. Discussion

Using a computational population of human atrial models, this study investigated the ionic determinants of conduction slowing and propagation failure elicited by progressively premature stimulation, identifying distinct ionic profiles associated with each conduction behavior.

Consistent with previous Population of Models studies [5], independent variation of ionic conductances generated a broad range of physiologically viable electrophysiological phenotypes, enabling identification of ionic combinations associated with distinct conduction responses to premature stimulation. Within the explored ionic parameter space, preserved conduction predominated, whereas conduction slowing and propagation failure emerged in a minority of models.

Partial correlation analysis confirmed the predominant role of g_{Na} in determining conduction velocity during steady-state pacing. During the initial response to premature stimulation, however, g_{K1} became the ionic parameter most strongly associated with conduction slowing. This suggests that membrane excitability, rather than baseline conduction properties, becomes the main determinant of conduction slowing as coupling intervals shorten.

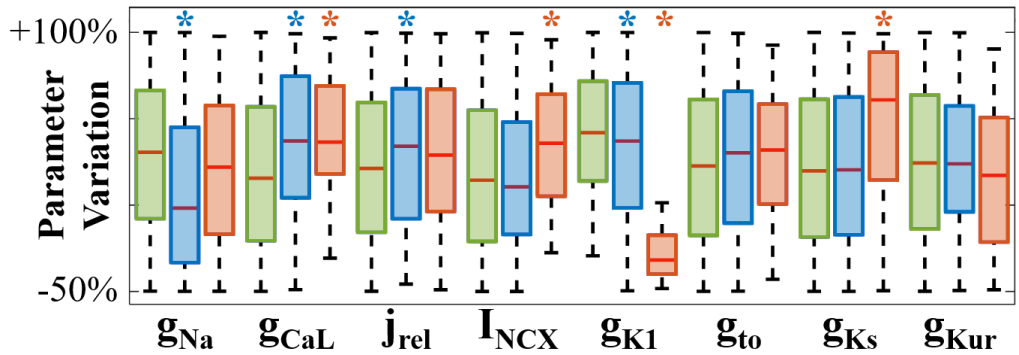

Figure 3. Distribution of the scaled ionic parameters in *NonDropPop* (green), *DropPop* (blue), and *FailPop* (orange). Asterisks denote statistically significant differences ($p < 0.05$, Mann–Whitney U test) compared with NonDropPop.

As coupling intervals were further shortened within the DropPop population, g_{K1} remained the ionic parameter most strongly associated with conduction slowing. However, as the tissue approached its limit of excitability, the influence of the depolarizing currents g_{Na} and g_{CaL} became more pronounced. This observation is consistent with previous computational studies highlighting the importance of the balance between sodium and calcium currents under conditions close to conduction failure [7].

DropPop models were characterized by reduced g_{Na} together with increased g_{CaL} and j_{Rel}. This ionic profile suggests a partial loss of depolarization reserve, increasing the susceptibility to conduction slowing during premature stimulation. Increases in g_{CaL} and j_{Rel} may represent compensatory mechanisms that help maintain excitability. The marked reduction in g_{K1} observed in FailPop suggests that loss of inward rectifier current is a key prerequisite for propagation failure. Interestingly, this ionic profile was accompanied by increased g_{CaL}, I_{NCX} and g_{Ks}. While the increases in g_{CaL} and I_{NCX} may reflect mechanisms that partially preserve depolarization under severely reduced excitability, the higher g_{Ks} may reflect an adaptive response associated with the profound reduction in g_{K1}.

Interestingly, the reductions in g_{Na} and g_{K1} observed in DropPop and FailPop are consistent with ionic changes reported in fibrosis-associated TGF-β1 remodeling [8]. In contrast, our population exhibited increased g_{CaL}, suggesting that enhanced calcium current may act as a compensatory mechanism that helps preserve excitability.

Despite these distinct ionic signatures, the functional consequences observed in homogeneous tissue remained relatively limited. Although DropPop models tended to exhibit lower conduction velocities than NonDropPop models, the additional conduction slowing induced by progressively premature stimulation remained relatively modest, with an average reduction of 5.3 cm/s between S2a and S2c. These findings suggest that ionic variability alone may not be sufficient to reproduce the marked conduction slowing commonly observed during functional mapping in patients.

However, the identification of models exhibiting complete propagation failure is particularly relevant, as these ionic profiles may act as localized conduction barriers when incorporated into heterogeneous tissue models. Future studies should investigate whether heterogeneous distributions of these ionic phenotypes can give rise to abnormal conduction patterns and electrogram fractionation during premature stimulation.

Acknowledgments

This work was funded by the Generalitat Valenciana grants CIAICO/2024/247, AICO/2021/318, and by grants PID2023-148702OB-I00, Beatriz Galindo program (grant BG24/00156) and EraNet PCI2024-153442 funded by MCIN/ 10.13039/501100011033 and by "ERDF A way of making Europe."

References

[1] A. S. Jadidi, E. Duncan, S. Miyazaki, N. Lellouche, A. J. Shah, A. Forclaz, et al. "Functional nature of electrogram fractionation demonstrated by left atrial high-density mapping". *Circ Arrhythm Electrophysiol*. vol. 5, no. 1, pp. 32–42, 2012.

[2] A. Redondo-Rodríguez, A. Ramos-Prada, J. G. Quintanilla, D. Calvo, J. Sánchez-González, D. Enríquez-Vázquez, et al., "Dispersion of activation in single-beat global maps during programmed ventricular stimulation identifies infarct-related ventricular tachycardia isthmus sites," *J. Am. Heart Assoc.*, vol. 13, no. 23, Art. no. e038441, 2024.

[3] E. Silva Garcia, I. Lobo-Torres, J. Fernández-Armenta, D. Penela, M. Fernandez-Garcia, A. Gomez-Lopez, et al., "Functional mapping to reveal slow conduction and substrate progression in atrial fibrillation," *EP Europace*, vol. 25, no. 11, Art. no. euad246, 2023.

[4] J. T. Koivumäki, T. Korhonen, and P. Tavi, "Impact of sarcoplasmic reticulum calcium release on calcium dynamics and action potential morphology in human atrial myocytes: A computational study," PLoS Comput. Biol., vol. 7, no. 1, Art. no. e1001067, 2011.

[5] O. J. Britton, A. Bueno-Orovio, K. Van Ammel, H. R. Lu, R. Towart, D. J. Gallacher, et al., "Experimentally calibrated population of models predicts and explains intersubject variability in cardiac cellular electrophysiology," *Proc. Natl. Acad. Sci. U. S. A.*, vol. 110, no. 23, pp. E2098–E2105, 2013.

[6] M. Holmes, H. Martinez-Navarro, M. Mohr, J. M. Chambard, V. Ballet, E. Vermersch, et al., "Quantitative assessment of the usability of electromechanical human-based modelling and simulation to replace Langendorff isolated rabbit heart experiments in the preclinical setting," Front. Pharmacol., vol. 16, Art. no. 1671199, 2025.

[7] A. Liberos, A. Bueno-Orovio, M. Rodrigo, U. Ravens, I. Hernandez-Romero, F. Fernandez-Aviles, M. S. Guillem, B. Rodriguez, and A. M. Climent, "Balance between sodium and calcium currents underlying chronic atrial fibrillation termination: An in silico intersubject variability study," *Heart Rhythm*, vol. 13, no. 12, pp. 2358–2365, 2016.

[8] C. H. Roney, J. D. Bayer, S. Zahid, M. Meo, P. M. Boyle, N. A. Trayanova, M. Haïssaguerre, R. Dubois, H. Cochet, and E. J. Vigmond, "Modelling methodology of atrial fibrosis affects rotor dynamics and electrograms," *Europace*, vol. 18, suppl. 4, pp. iv146–iv155, 2016.

Address for correspondence:

Alejandro Liberos;
Av. de la Universitat s/n 46100 Burjassot (Valencia, Spain).
alejandro.liberos@uv.es